Nuclear-Electronic Orbital Multistate Density Functional Theory

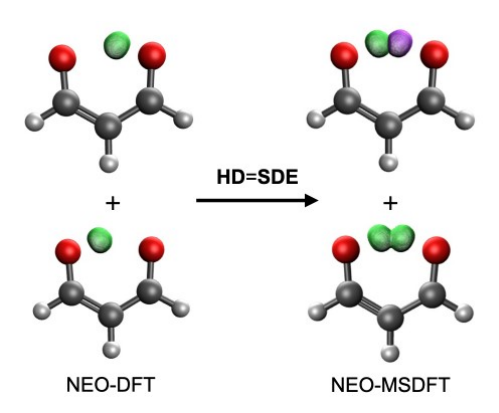
Qi Yu and Sharon Hammes-Schiffer*

Department of Chemistry, Yale University, 225 Prospect Street, New Haven, Connecticut 06520 USA *Corresponding author email: sharon.hammes-schiffer@yale.edu

Abstract

Hydrogen tunneling is essential for a wide range of chemical and biological processes. The description of hydrogen tunneling with multicomponent quantum chemistry approaches, where the transferring hydrogen nucleus is treated on the same level as the electrons, is challenging due to the importance of both static and dynamical electron-proton correlation. Herein the nuclear-electronic orbital multistate density functional theory (NEO-MSDFT) method is presented as a strategy to include both types of correlation. In this approach, two localized nuclear-electronic wave functions obtained with the NEO-DFT method are combined with a nonorthogonal configurational interaction approach to produce bilobal, delocalized ground and excited vibronic states. By including a correction function, the NEO-MSDFT approach can produce quantitatively accurate hydrogen tunneling splittings for fixed geometries of systems such as malonaldehyde and acetoacetaldehyde. This approach is computationally efficient and can be combined with methods such as vibronic coupling theory to describe tunneling dynamics and to compute vibronic couplings in many types of systems.

TOC Graphic



Hydrogen tunneling plays an important role in many biological and chemical processes. ¹⁻³ A variety of approaches have been developed to describe hydrogen tunneling, such as path integral, ³⁻⁶ multiconfigurational time-dependent Hartree (MCTDH), ⁷⁻⁹ and diffusion Monte Carlo (DMC) ¹⁰⁻¹² methods. However, these conventional approaches typically require extensive single-point energy calculations on Born-Oppenheimer potential energy surfaces and can be computationally prohibitive for large molecular systems. The nuclear-electronic orbital (NEO) method provides a robust and computationally efficient framework that treats specified nuclei, typically protons, quantum mechanically on the same level as the electrons. ¹³⁻¹⁴ This multicomponent quantum chemistry approach avoids the Born-Oppenheimer separation between the electrons and the quantum nuclei. In the application of the NEO method to hydrogen transfer systems, the transferring hydrogen nucleus and all electrons are treated quantum mechanically. The description of hydrogen tunneling within this framework is challenging because the nuclear-electronic wave function tends to localize in one well of a symmetric double-well potential energy surface without inclusion of sufficient static and dynamical electron-proton correlation. ¹⁵⁻¹⁶

Within the NEO framework, the nonorthogonal configuration interaction (NEO-NOCI) approach was developed ¹⁷ in an effort to obtain the tunneling splittings in molecular systems undergoing hydrogen tunneling. This approach constructs ground and excited state bilobal, delocalized nuclear-electronic wave functions through linear combinations of two nonorthogonal localized wave functions calculated at the NEO Hartree-Fock (NEO-HF) level of theory. The corresponding tunneling splitting is obtained from the energy difference between the ground and first excited state energies. However, because the NEO-HF method does not include electron-proton and electron-electron dynamical correlation, which are known to be important, the protonic wave functions are much too localized and cannot produce even qualitatively reasonable tunneling

splittings. Thus, a multicomponent method that incorporates sufficient correlation effects and provides accurate proton densities is needed to compute reliable hydrogen tunneling splittings.

Density functional theory (DFT) approaches have also been developed within the NEO framework. The NEO-DFT method includes dynamical electron-electron correlation using standard electronic exchange-correlation functionals while also including dynamical electron-proton correlation using an electron-proton correlation functional such as epc17-2 or epc-19. This approach has been shown to provide accurate proton densities, energies, and optimized geometries at relatively low computational cost with scaling of N^4 , where N is the number of basis functions. In this Letter, we present the NEO multistate density functional theory (NEO-MSDFT) method, which combines aspects of NEO-NOCI and NEO-DFT and therefore includes both static and dynamical correlation. Our applications of this theory show that the NEO-MSDFT method is able to provide accurate hydrogen tunneling splittings and bilobal, delocalized proton densities for different types of molecular systems.

The basic scheme of NEO-MSDFT is analogous to the MSDFT developed in the context of conventional electronic structure calculations. $^{22\text{-}24}$ Given a double-well potential energy surface, two localized nuclear-electronic wave functions, $|\Psi_{\text{I}}\rangle$ and $|\Psi_{\text{II}}\rangle$, are obtained from the variational NEO-DFT solutions with each nuclear wave function centered at the minimum of one well. Specifically, $|\Psi_{\text{I}}\rangle = \Phi_{\text{I}}^e \Phi_{\text{I}}^p$ is localized in the left well, and $|\Psi_{\text{II}}\rangle = \Phi_{\text{II}}^e \Phi_{\text{II}}^p$ is localized in the right well from the variational procedure using two different initial wave functions. These localized wave functions are products of Kohn-Sham electronic and protonic determinants, Φ^e and Φ^p , which are composed of electronic and protonic orbitals, respectively. The ground and excited state NEO-MSDFT wave functions are linear combinations of these localized wave functions:

$$\begin{aligned} \left| \Psi_{0} \right\rangle &= D_{\mathrm{I}}^{0} \left| \Psi_{\mathrm{I}} \right\rangle + D_{\mathrm{II}}^{0} \left| \Psi_{\mathrm{II}} \right\rangle \\ \left| \Psi_{1} \right\rangle &= D_{\mathrm{I}}^{1} \left| \Psi_{\mathrm{I}} \right\rangle + D_{\mathrm{II}}^{1} \left| \Psi_{\mathrm{II}} \right\rangle \end{aligned} \tag{1}$$

The coefficients in Equation (1) are determined by solving the 2×2 NEO-MSDFT matrix equation:

$$\mathbf{HD} = \mathbf{SDE} \tag{2}$$

Here H is the effective Hamiltonian given by

$$\mathbf{H} = \begin{bmatrix} H_{\mathrm{I,I}} & H_{\mathrm{I,II}} \\ H_{\mathrm{II,I}} & H_{\mathrm{II,II}} \end{bmatrix} \tag{3}$$

where the Hamiltonian matrix elements are defined below, and **S** is the overlap matrix between the two localized states:

$$\mathbf{S} = \begin{bmatrix} S_{I,I} & S_{I,II} \\ S_{II,I} & S_{II,II} \end{bmatrix} = \begin{bmatrix} 1 & \langle \Psi_I | \Psi_{II} \rangle \\ \langle \Psi_{II} | \Psi_I \rangle & 1 \end{bmatrix}$$
(4)

The off-diagonal matrix elements of the overlap matrix are given by

$$S_{I,II} = S_{II,I} = \left\langle \Psi_{I} \middle| \Psi_{II} \right\rangle = \left\langle \Phi_{I}^{e} \Phi_{I}^{p} \middle| \Phi_{II}^{e} \Phi_{II}^{p} \right\rangle = S_{I,II}^{e} S_{I,II}^{p}$$

$$S_{I,II}^{e} = \det[(\mathbf{C}_{I,o}^{e})^{T} \mathbf{S}^{e} (\mathbf{C}_{II,o}^{e})]$$

$$S_{I,II}^{p} = \det[(\mathbf{C}_{I,o}^{p})^{T} \mathbf{S}^{p} (\mathbf{C}_{II,o}^{p})]$$
(5)

where $\mathbf{C}_{I,o}^e/\mathbf{C}_{I,o}^p$ and $\mathbf{C}_{II,o}^e/\mathbf{C}_{II,o}^p$ are the coefficients of the occupied electronic/protonic Kohn-Sham orbitals for states I and II, respectively, and \mathbf{S}^e and \mathbf{S}^p are the overlap matrices of the electronic and protonic basis functions, respectively.

The tunneling splitting for a double well potential energy surface can be represented as the energy difference between the ground and first excited vibronic state energies obtained by solving Equation (2). The associated analytical expression for this splitting is

$$\Delta E_{01} = \frac{1}{1 - S_{I,II}^2} \sqrt{(H_{I,I} - H_{II,II})^2 (1 - S_{I,II}^2) + \left[2H_{I,II} - (H_{I,I} + H_{II,II})S_{I,II}\right]^2}$$
(6)

Moreover, the analytical expression for the vibronic coupling²⁵⁻²⁶ between the two symmetrically orthogonalized localized nuclear-electronic states is

$$V = \frac{1}{1 - S_{\text{I,II}}^2} \left| H_{\text{I,II}} - \frac{(H_{\text{I,I}} + H_{\text{II,II}})}{2} S_{\text{I,II}} \right|$$
 (7)

For symmetric systems, the vibronic coupling in Eq. (7) is half the magnitude of the tunneling splitting in Eq. (6).

The NEO Hamiltonian \hat{H}_{NEO} includes the kinetic energies of the electrons and quantum nuclei, as well as all of the Coulomb integrals between pairs of electrons, quantum nuclei, and classical nuclei. In NEO-MSDFT, the diagonal matrix elements of the effective Hamiltonian given in Equation (3) are simply the NEO-DFT energies of the corresponding NEO Kohn-Sham (NEO-KS) determinants. Thus, $H_{\text{I,I}} = E_{\text{I}}^{\text{NEO-DFT}} \left[\rho_{\text{I}}^{\text{e}}, \rho_{\text{I}}^{\text{p}} \right]$ and $H_{\text{II,II}} = E_{\text{II}}^{\text{NEO-DFT}} \left[\rho_{\text{II}}^{\text{e}}, \rho_{\text{II}}^{\text{p}} \right]$, where $\rho_{\text{I}}^{\text{e}} / \rho_{\text{I}}^{\text{p}}$ and $\rho_{\text{II}}^{\text{e}} / \rho_{\text{II}}^{\text{p}}$ are the electronic/protonic densities for states I and II, respectively, obtained from the NEO-KS determinants. The off-diagonal matrix elements can be obtained from wave function-based methods such as NEO-NOCI in a straightforward manner. In the Kohn-Sham DFT framework, however, the off-diagonal matrix elements are not well-defined.²³

Analogous to the conventional electronic structure MSDFT approach of Gao and coworkers, ²³ the off-diagonal elements can be approximated by

$$H_{I,II} = \langle \Psi_{I} | \hat{\boldsymbol{H}}_{NEO} | \Psi_{II} \rangle + \frac{\lambda}{2} S_{I,II} \left(E_{I}^{corr} + E_{II}^{corr} \right)$$

$$= S_{I,II} \left(E_{nuc} + Tr \left[\mathbf{P}_{I,II}^{e} \mathbf{h}^{e} \right] + Tr \left[\mathbf{P}_{I,II}^{p} \mathbf{h}^{p} \right] + \frac{1}{2} Tr \left[\mathbf{P}_{I,II}^{e} \mathbf{J}^{ee} \mathbf{P}_{I,II}^{e} \right] + \frac{1}{2} Tr \left[\mathbf{P}_{I,II}^{p} \mathbf{J}^{pp} \mathbf{P}_{I,II}^{p} \right]$$

$$- Tr \left[\mathbf{P}_{I,II}^{e} \mathbf{J}^{ep} \mathbf{P}_{I,II}^{p} \right] - \frac{1}{4} Tr \left[\mathbf{P}_{I,II}^{e} \mathbf{K}^{ee} \mathbf{P}_{I,II}^{e} \right] - \frac{1}{2} Tr \left[\mathbf{P}_{I,II}^{p} \mathbf{K}^{pp} \mathbf{P}_{I,II}^{p} \right] + \frac{\lambda}{2} S_{I,II} \left(E_{I}^{corr} + E_{II}^{corr} \right)$$

$$(8)$$

In this first equality of Equation (8), $\langle \Psi_{\rm I} | \hat{H}_{\rm NEO} | \Psi_{\rm II} \rangle$ is the energy computed at the NEO-HF level with the NEO-KS determinants, $S_{\rm I,II}$ is the overlap between the two NEO-KS determinants as defined in Equation (5), and the correlation energy $E_{\rm I}^{\rm corr}$ or $E_{\rm II}^{\rm corr}$ is calculated as the difference between the NEO-DFT and NEO-HF energies for state I or II, respectively:

$$E_{\mathrm{I}}^{\mathrm{corr}} = E_{\mathrm{I}}^{\mathrm{NEO-DFT}} \left[\rho_{\mathrm{I}}^{\mathrm{e}}, \rho_{\mathrm{I}}^{\mathrm{p}} \right] - E_{\mathrm{I}}^{\mathrm{NEO-HF}} \left[\rho_{\mathrm{I}}^{\mathrm{e}}, \rho_{\mathrm{I}}^{\mathrm{p}} \right]$$

$$E_{\mathrm{II}}^{\mathrm{corr}} = E_{\mathrm{II}}^{\mathrm{NEO-DFT}} \left[\rho_{\mathrm{II}}^{\mathrm{e}}, \rho_{\mathrm{II}}^{\mathrm{p}} \right] - E_{\mathrm{II}}^{\mathrm{NEO-HF}} \left[\rho_{\mathrm{II}}^{\mathrm{e}}, \rho_{\mathrm{II}}^{\mathrm{p}} \right]$$
(9)

In the second equality of Equation (8), which assumes a closed-shell electronic and high-spin protonic system, \mathbf{h} , \mathbf{J} , and \mathbf{K} represent the core Hamiltonian, Coulomb, and exchange terms, respectively, for electrons and protons, and $\mathbf{P}_{I,II}^{e}$ and $\mathbf{P}_{I,II}^{p}$ are the transition density matrices between states I and II defined by

$$\mathbf{P}_{\mathbf{I},\mathbf{II}}^{e} = \mathbf{C}_{\mathbf{I},o}^{e} [(\mathbf{C}_{\mathbf{I},o}^{e})^{\mathsf{T}} \mathbf{S}^{e} (\mathbf{C}_{\mathbf{I},o}^{e})]^{-1} (\mathbf{C}_{\mathbf{I},o}^{e})^{\mathsf{T}}$$

$$\mathbf{P}_{\mathbf{I},\mathbf{II}}^{p} = \mathbf{C}_{\mathbf{I},o}^{p} [(\mathbf{C}_{\mathbf{I},o}^{p})^{\mathsf{T}} \mathbf{S}^{p} (\mathbf{C}_{\mathbf{I},o}^{p})]^{-1} (\mathbf{C}_{\mathbf{I},o}^{p})^{\mathsf{T}}$$
(10)

The parameter λ in Equation (8) is used as a correction of the correlation energy and can be parametrized by fitting experimental data.^{23, 27} In this work, we use $\lambda = 1$ in all NEO-MSDFT calculations. This form of the off-diagonal matrix elements ensures that the vibronic coupling given in Equation (7) is the same as the NEO-NOCI coupling using the NEO-KS determinants.

An alternative form of the off-diagonal Hamiltonian matrix element developed in the context of conventional electronic structure theory uses the symmetrized transition density matrix to evaluate the exchange-correlation energies.²⁸ We also employed this alternative strategy, which we denote as NEO-MSDFT2. The symmetrized electronic and protonic transition density matrices are defined as

$$\tilde{I} = \frac{e}{2} \left(\mathbf{C}_{I,o}^{e} [(\mathbf{C}_{I,o}^{e})^{T} \mathbf{S}^{e} (\mathbf{C}_{I,o}^{e})]^{-1} (\mathbf{C}_{II,o}^{e})^{T} + \mathbf{C}_{II,o}^{e} [(\mathbf{C}_{I,o}^{e})^{T} \mathbf{S}^{e} (\mathbf{C}_{II,o}^{e})]^{-1} (\mathbf{C}_{I,o}^{e})^{T} \right) \\
= \frac{1}{2} \left(\mathbf{C}_{I,o}^{p} [(\mathbf{C}_{II,o}^{p})^{T} \mathbf{S}^{p} (\mathbf{C}_{I,o}^{p})]^{-1} (\mathbf{C}_{II,o}^{p})^{T} + \mathbf{C}_{II,o}^{p} [(\mathbf{C}_{I,o}^{p})^{T} \mathbf{S}^{p} (\mathbf{C}_{II,o}^{p})]^{-1} (\mathbf{C}_{I,o}^{p})^{T} \right)$$
(11)

In the multicomponent extension of this approach, the off-diagonal element is expressed as

$$H_{I,II} = S_{I,II} \left(\operatorname{Tr} \left[\mathbf{P}_{I,II}^{e} \mathbf{h}^{e} \right] + \frac{1}{2} \operatorname{Tr} \left[\mathbf{P}_{I,II}^{e} \mathbf{J}^{ee} \mathbf{P}_{I,II}^{e} \right] + \operatorname{Tr} \left[\mathbf{P}_{I,II}^{p} \mathbf{h}^{p} \right] + \frac{1}{2} \operatorname{Tr} \left[\mathbf{P}_{I,II}^{p} \mathbf{J}^{pp} \mathbf{P}_{I,II}^{p} \right] - \operatorname{Tr} \left[\mathbf{P}_{I,II}^{e} \mathbf{J}^{ep} \mathbf{P}_{I,II}^{p} \right]$$

$$- \frac{a}{4} \operatorname{Tr} \left[\mathbf{P}_{I,II}^{e} \mathbf{K}^{ee} \mathbf{P}_{I,II}^{e} \right] - \frac{1}{2} \operatorname{Tr} \left[\mathbf{P}_{I,II}^{p} \mathbf{K}^{pp} \mathbf{P}_{I,II}^{p} \right] + E_{exc} \left[\tilde{I} \right]$$

$$(12)$$

Here $E_{\rm exc}$, $E_{\rm pc}$, and $E_{\rm epc}$ are the electronic exchange-correlation, proton-proton correlation, and electron-proton correlation functionals, respectively, assuming full proton-proton exchange with high-spin protons. The parameter a is determined by the selected electronic exchange-correlation functional. Note that the transition density is not positive definite, and therefore utilizing it as the argument of the exchange-correlation functionals could be problematic, although we did not encounter difficulties in the calculations presented herein.

The NEO-MSDFT approach includes dynamical correlation in the localized nuclear-electronic wave functions $|\Psi_{\rm I}\rangle$ and $|\Psi_{\rm II}\rangle$ with NEO-DFT and static correlation through the two-state NEO-NOCI expansion. As discussed elsewhere, typically the variational solution for a single configurational nuclear-electronic wave function in a symmetric double-well potential associated with hydrogen transfer is localized in one well rather than delocalized over both wells. This behavior is opposite to that observed for electronic wave functions in electron transfer systems, where the wave function tends to delocalize and requires constraints to localize the charge or spin. This qualitatively different behavior for nuclear-electronic wave functions is mainly due to the attractive electron-proton Coulomb interaction in contrast to the repulsive electron-electron Coulomb interaction. For this reason, the localized nuclear-electronic wave functions $|\Psi_{\rm I}\rangle$ and

 $|\Psi_{II}\rangle$ can be obtained using NEO-HF without any constraints. However, our previous work on systems in which the hydrogen moves in single-well potentials, such as HCN and FHF⁻, has shown that the nuclear wave function is much too localized at the NEO-HF level. ¹⁹⁻²⁰ This previous work illustrated that the inclusion of electron-proton dynamical correlation with NEO-DFT using the epc17 functionals significantly delocalizes the nuclear wave function and improves the agreement with numerically exact results for these types of systems. ¹⁹⁻²⁰ On the other hand, the NEO-DFT/epc17-2 approach still produces nuclear-electronic wavefunctions that are localized in a single well of a symmetric double-well potential associated with hydrogen transfer, presumably mainly due to the lack of static correlation.

Thus, the use of NEO-DFT to provide suitably delocalized nuclear-electronic wavefunctions within each well in conjunction with NEO-NOCI to produce a bilobal, delocalized wave function over both wells for hydrogen transfer systems combines dynamical and static correlation in a physically reasonable manner. In general, dynamical and static correlation are not strictly separable, and therefore double counting of these correlation effects²⁹ could be problematic with certain density functionals. Nevertheless, the physical properties of the nuclear-electronic wave functions produced using NEO-DFT/epc17-2 and the simple two-state CI expansion, as well as the accuracy of the hydrogen tunneling splittings given below, indicate that such double counting is not a significant problem for this implementation of the NEO-MSDFT approach.

The steps of a NEO-MSDFT calculation for a given molecule with fixed geometry are summarized in Figure S1 of the Supporting Information (SI). The transferring hydrogen nucleus is represented by two proton basis function centers each containing both electronic and protonic basis functions. In the first step, the positions of the proton basis function centers are optimized at the NEO-DFT level by performing two separate optimizations, each with a single basis function

center corresponding to the hydrogen on either side. Note that all classical nuclei remained fixed during these basis function center optimizations. For a symmetric double-well system, only one optimization is required because the other position can be determined according to symmetry. The remainder of the calculation includes both basis function centers fixed at these optimized positions. In the second step, two single-point NEO-DFT calculations are performed with the hydrogen localized on each side. In the third step, the NEO-KS determinants from these NEO-DFT calculations are used for the NEO-MSDFT calculations as described above.

We implemented the NEO-MSDFT method in a development version of the Q-Chem 5.3 package.³⁰ Tests were carried out by calculating tunneling splittings and proton densities for the following molecular systems: FHF-, OCHCO+, benzyl/toluene, malonaldehyde, and acetoacetaldehyde. For FHF⁻ and OCHCO⁺, the potential energy curve along the proton transfer coordinate at their equilibrium geometries is either a single-well potential or a double-well potential with a low barrier.³¹⁻³² To investigate the applicability of NEO-MSDFT for hydrogen tunneling systems, however, we selected different nonequilibrium geometries corresponding to larger F–F or C–C distances and calculated the tunneling splittings at these fixed nonequilibrium geometries. For each geometry of each molecule, the reference tunneling splitting and proton densities were obtained with the Fourier grid Hamiltonian (FGH) method, 33 where the threedimensional (3D) Schrödinger equation was solved for a proton moving on a 3D potential energy surface computed on a grid. The FGH method is numerically exact for electronically adiabatic systems and can be treated as an accurate reference for the systems studied herein. Additional computational details about the NEO-MSDFT and FGH calculations, as well as the Cartesian coordinates of the five molecules, are given in the SI.

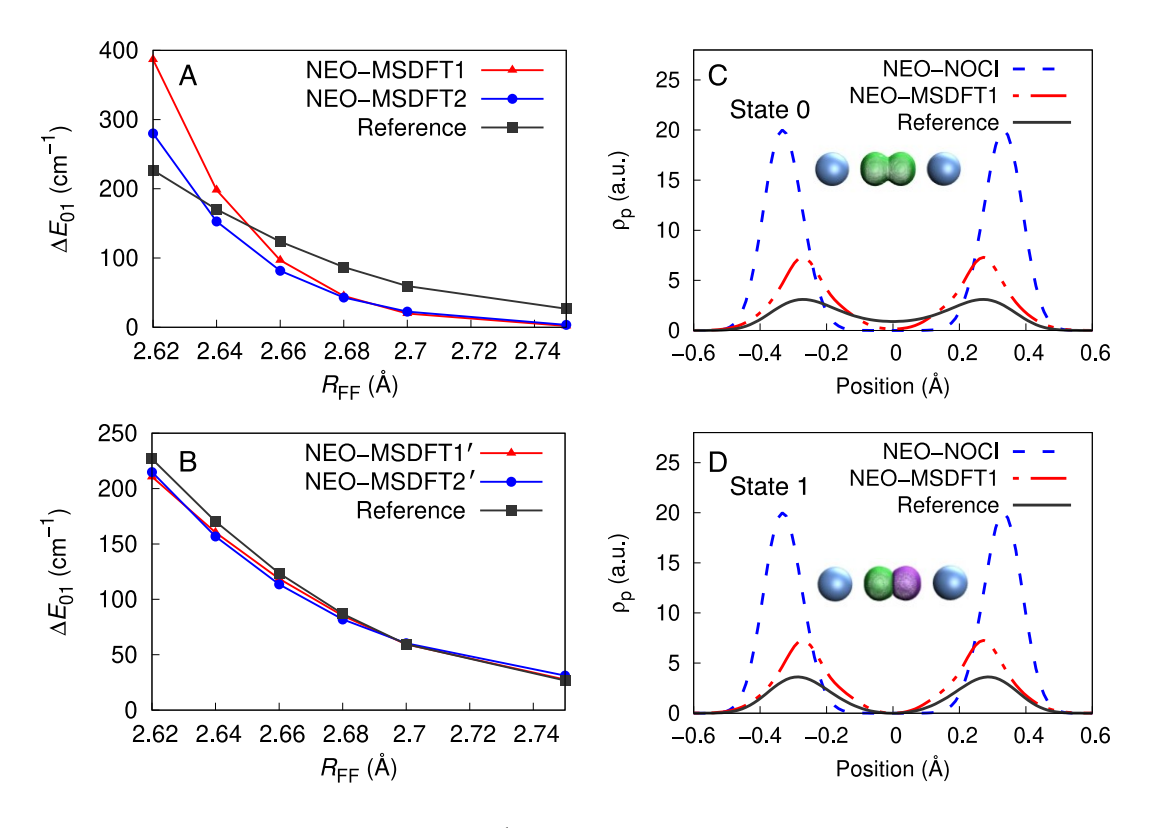


Figure 1. (A-B) Tunneling splittings (cm⁻¹) for the FHF⁻ molecule at different fixed F–F distances calculated with the (A) NEO-MSDFT, NEO-MSDFT2, and reference FGH methods and (B) NEO-MSDFT', NEO-MSDFT2', and reference FGH methods. (C-D) One-dimensional slices of the ground and first-excited state proton densities of FHF⁻ along the proton transfer axis with the F–F distance set to 2.66 Å as obtained with the NEO-NOCI, NEO-MSDFT, and reference FGH methods. The 3D proton wave functions obtained with the NEO-MSDFT method are also plotted in each panel.

Figure 1A shows the tunneling splittings of FHF⁻ with different fixed F–F distances calculated with the NEO-MSDFT, NEO-MSDFT2, and reference FGH methods. The NEO calculations were performed at the NEO-DFT/B3LYP/epc17-2 level of theory with electronic basis sets aug-cc-pVDZ for the classical nuclei and aug-cc-pV5Z³⁴ for the quantum proton, as well as the protonic basis set PB5-G.³⁵ The aug-cc-pV5Z basis set for the quantum proton was chosen based on previous studies indicating that relatively large electronic basis sets are required to obtain accurate proton vibrational excitation energies.³⁶⁻³⁷ Basis set convergence tests are provided in Figures S2 and S3 of the SI. The 3D grid potential for the FGH method was generated from

DFT/B3LYP/aug-cc-pVDZ single-point energy calculations. As the F–F distance increases, the tunneling splitting decreases monotonically due to the increasing barrier height of the double-well potential. However, neither NEO-MSDFT nor NEO-MSDFT2 quantitatively reproduces the correct tunneling splittings compared to the reference values. This discrepancy arises mainly from slight over-localization of the two protonic wave functions, Φ_I^P and Φ_{II}^P , leading to an overlap between these two wave functions that is somewhat too small. As shown previously¹⁹⁻²⁰ and in Figure S4, the proton densities associated with the NEO-MSDFT/epc17-2 method, which includes electron-proton correlation via the epc17-2 functional, are significantly improved compared to those associated with the NEO-NOCI method, which treats the nonorthogonal localized wave functions at the NEO-HF level. In principle, the protonic wave functions could be further improved by using a more accurate electron-proton correlation functional, but such a functional is not available at this time.

To account for this limitation of the electron-proton correlation functional and the resulting inaccuracies in the overlap between the two localized nuclear-electronic wave functions, we applied a simple correction to the overlap $S_{\rm LII}$. The corrected overlap is of the form

$$S_{\text{I,II}}^{\text{corr}} = \alpha (S_{\text{I,II}})^{\beta} \tag{13}$$

where $\alpha = 0.0604$ and $\beta = 0.492$ for NEO-MSDFT and $\alpha = 0.1534$ and $\beta = 0.628$ for NEO-MSDFT2. The corrected tunneling splitting was calculated using this corrected overlap term in Equations (6), (8) and (12), although it was not used in the transition densities given by Eq. (10). The values of α and β were determined by fitting the calculated tunneling splitting data for the FHF⁻ molecule with different F–F distances to the reference FGH data. These parameters can be modified when different electron-proton correlation functionals are used. Throughout this Letter, these parameters remain unchanged in order to test the transferability of the NEO-MSDFT method

across different molecules. The modified NEO-MSDFT and NEO-MSDFT2 methods for tunneling splittings computed with the corrected overlap term are denoted NEO-MSDFT' and NEO-MSDFT2', respectively. As shown in Figure 1B, the resulting tunneling splittings agree very well with the FGH reference data for both the NEO-MSDFT' and NEO-MSDFT2' methods.

The one-dimensional (1D) proton densities along the proton transfer axis and the 3D proton wave functions for the ground and excited states of FHF⁻ with an F–F distance of 2.66 Å are depicted in Figures 1C and 1D. In addition to these NEO-MSDFT proton densities, the 1D proton densities calculated with the NEO-NOCI method are also shown for comparison. For both the ground and excited states, the NEO-MSDFT method produces significantly delocalized proton densities over the two wells and agrees reasonably well with the FGH reference results. However, the ground state proton density is too small in the central region, mainly due to insufficient overlap between the two localized proton densities. Nevertheless, the NEO-MSDFT results are shown to be a significant improvement over the NEO-NOCI results, where the proton densities are highly overlocalized and shifted outward. This improvement arises from the additional electron-proton dynamical correlation included in the NEO-DFT/epc17-2 method compared to the NEO-HF method (Figure S4). ¹⁹⁻²¹ The 3D plots of the protonic wave function in Figure 1 also confirm that the ground state proton wave function delocalizes over the two wells and that the first excited state proton wave function exhibits a node at the midpoint.

Next we used the NEO-MSDFT scheme to compute the tunneling splittings and proton densities for other systems. Figure 2 shows the tunneling splittings for the OCHCO⁺ and benzyl/toluene systems for varying C–C distances, computed with the NEO-MSDFT' and NEO-MSDFT2' methods as well as the FGH reference method. The tunneling splittings and 1D proton densities computed without the corrected overlap term are given in Tables S2-S3 and Figure S5.

For OCHCO⁺, the calculations were performed with the same functionals and basis sets as for the FHF⁻ molecule. As seen from Figure 2, the tunneling splittings computed with the NEO-MSDFT' method agree very well with the FGH reference data for OCHCO⁺. The results computed with the NEO-MSDFT2' method also behave reasonably well. Tests using different electronic functionals, including BLYP, PBE, PBE0, and ω B97X-D, were also conducted for both the FHF⁻ and OCHCO⁺ molecules (Figures S6-S9), showing reasonable transferability across electronic functionals.

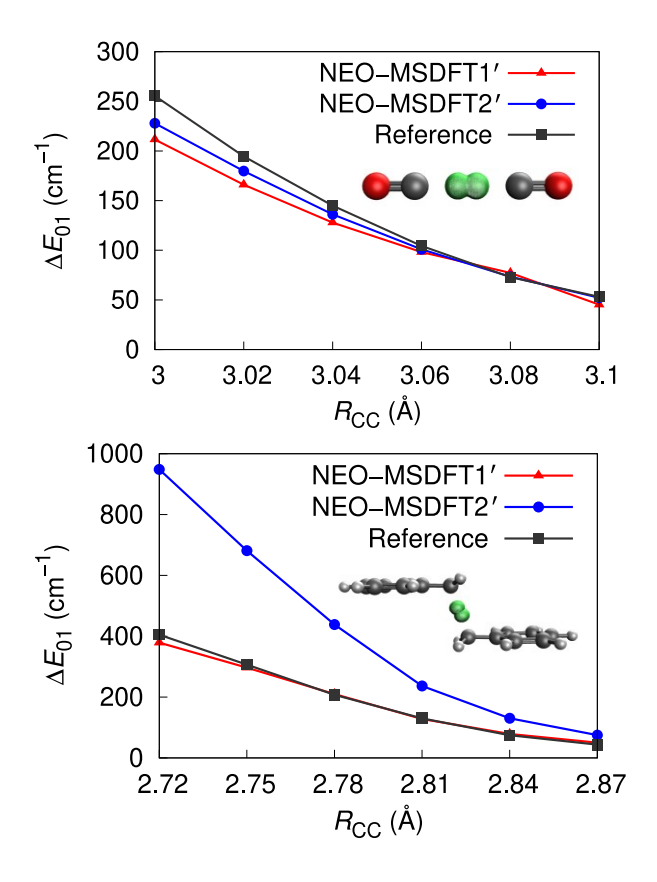


Figure 2. Tunneling splittings (cm⁻¹) for the OCHCO⁺ (upper panel) and benzyl/toluene (lower panel) systems at different fixed C–C distances calculated with the NEO-MSDFT', NEO-MSDFT2', and reference FGH methods. Representative 3D ground state proton wave functions obtained with the NEO-MSDFT method are also plotted for each molecule.

For the benzyl/toluene system, we used the range-separated hybrid ω B97X-D functional³⁸ with the electronic basis sets cc-pVDZ for the classical nuclei and cc-pV5Z for the quantum proton, as well as the protonic basis set PB5-G. Other hybrid functionals, including B3LYP and PBE0, were also tested and exhibit similar behavior (Figures S10-S11). Figure 2 shows the results using the ω B97X-D functional as well as the FGH reference results conducted on 3D grids computed at the ω B97X-D/cc-pVDZ level of theory. Again, the NEO-MSDFT' method produced hydrogen tunneling splittings in very good agreement with the FGH reference data. However, the tunneling splittings computed with the NEO-MSDFT2' method are not in good agreement with the FGH reference data for the benzyl-toluene system, although the agreement is slightly better for other electronic functionals (Figures S10 and S11). Thus, the NEO-MSDFT' method appears to be stable and transferable across different molecules using different electronic functionals, whereas the NEO-MSDFT2' method appears to be less transferable, although this property may depend on the electron-proton correlation functional as well as the form of the correction function.

We also used the NEO-MSDFT method to compute the tunneling splittings and proton densities for malonaldehyde and acetoacetaldehyde, which are more complex molecules. The calculation of accurate tunneling splittings comparable to experiments requires the inclusion of coupling between the hydrogen and other molecular modes for these molecules. 11, 39 For the purposes of benchmarking the NEO-MSDFT method, however, we studied hydrogen tunneling between the two oxygen atoms for fixed geometries of these two molecules. The NEO calculations for malonaldehyde and acetoacetaldehyde were performed at the NEO-DFT/B3LYP/epc17-2 level of theory with the electronic basis sets cc-pVDZ for the classical nuclei and cc-pV5Z for the quantum proton, as well as the protonic basis set PB5-G. The FGH calculations were performed on a 3D grid potential computed at the B3LYP/cc-pVDZ level.

The ground and excited state proton densities for malonaldehyde and acetoacetaldehyde calculated with the NEO-NOCI, NEO-MSDFT, and FGH methods are presented in Figure 3. As shown in Figures 3A and 3B, the NEO-MSDFT ground and excited state proton densities for malonaldehyde are qualitatively similar to the FHF⁻ case in Figures 1C and 1D. The NEO-MSDFT approach produces delocalized proton densities for both ground and excited states, in good agreement with the FGH method, while the NEO-NOCI method produces proton densities that are much too localized. The acetoacetaldehyde molecule is different from all of the previous examples because the hydrogen moves in a slightly asymmetric double well potential due to the molecular asymmetry. Figures 3C and 3D illustrate that the NEO-NOCI method cannot even reproduce the double peak features of the proton densities. In contrast, the NEO-MSDFT method is able to produce asymmetric proton densities across the two wells and is in good agreement with the reference FGH results.

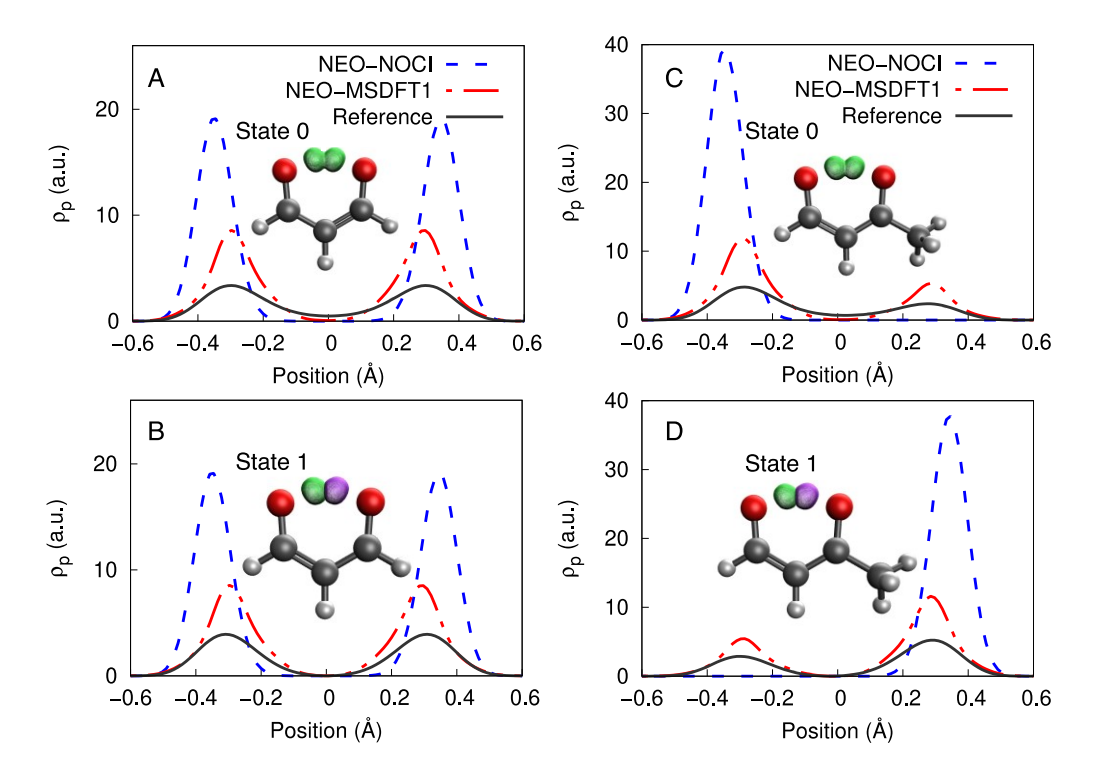


Figure 3. The ground and first excited state proton densities calculated with the NEO-NOCI, NEO-MSDFT, and reference FGH methods for malonaldehyde (A,B) and acetoacetaldehyde (C,D). The

1D slices were obtained along the proton transfer axis, which was chosen as the line connecting the optimized positions of the transferring hydrogen on each oxygen from B3LYP/cc-pVDZ calculations. The 3D proton wave functions calculated with the NEO-MSDFT method are also plotted in each panel.

The tunneling splittings computed with the NEO-MSDFT' and NEO-MSDFT2' methods for malonaldehyde and acetoacetaldehyde, as well as for the other three systems at selected geometries, are summarized in Table 1. The results for other geometries and the tunneling splittings computed without the corrected overlap term are given in Tables S1-S4. The NEO-MSDFT' and NEO-MSDFT2' methods predict accurate tunneling splittings for the systems investigated, although the NEO-MSDFT' method appears to be more stable and transferable. Note that the accuracy of the vibronic coupling is the same as the accuracy of the tunneling splitting for symmetric systems because they are related by a factor of two.

Table 1. Tunneling Splittings (cm⁻¹) of Five Systems Calculated with Different Methods.^a

System	Tunneling splitting		
	NEO-MSDFT'	NEO-MSDFT2'	FGH
FHF ⁻	85.3	81.9	86.9
OCHCO ⁺	100.9	104.5	98.1
benzyl/toluene	50.3	74.9	43.7
malonaldehyde	88.7	88.8	92.0
acetoacetaldehyde	101.1	92.9	107.4

^aThe results were obtained with a fixed F-F distance of 2.68 Å for FHF⁻, a fixed C-C distance of 3.06 Å for OCHCO⁺, and a fixed C-C distance of 2.87 Å for benzyl/toluene. The NEO results were obtained with the NEO-MSDFT' and NEO-MSDFT2' methods, which include a correction function to the overlap term. Results with other geometries and the uncorrected tunneling splittings are given in Tables S1-S4.

This Letter presents the NEO-MSDFT approach, which includes both static and dynamical correlation and enables the computationally efficient calculation of accurate proton densities and

hydrogen tunneling splittings for molecular systems. In this approach, two localized nuclear-electronic Kohn-Sham wave functions are obtained with the NEO-DFT method, and a nonorthogonal configuration interaction method is used to mix these two states to produce the bilobal, delocalized ground and excited states. The inclusion of electron-proton correlation is found to be important for the calculation of accurate proton wave functions. To account for limitations of the available electron-proton correlation functionals and the approximate form of the off-diagonal Hamiltonian matrix element, a correction function was applied to the overlap term to produce quantitatively accurate tunneling splittings. The same correction function was used for all systems. Such a correction function may not be necessary when more accurate electron-proton correlation functionals become available.

The NEO-MSDFT approach can be applied to a wide range of other systems, including those involving multiple protons, such as formic acid dimer and porphycene. Although this work shows that the NEO-MSDFT method is able to predict accurate tunneling splittings and proton densities for fixed geometries, the calculation of tunneling splittings that are comparable to experimental measurements requires the inclusion of the coupling between the hydrogen motion and other nuclear motions. For this purpose, the NEO-MSDFT method can be combined with approaches such as vibronic coupling theory. In comparison to other methods that require a large number of single-point energy calculations to compute 3D nuclear wave functions, the NEO-MSDFT approach is more computationally efficient because it requires only two single-point NEO-DFT calculations after identifying the proton basis function center positions. Another advantage of the NEO-MSDFT approach is that it provides the vibronic couplings in the adiabatic and nonadiabatic limits, as well as the intermediate regime. Thus, this work provides the foundation for a wide range of future directions.

Acknowledgement

The authors thank Zhen Tao, Dr. Fabijan Pavošević, and Dr. Evgeny Epifanovsky for help with the Q-Chem implementation. The authors also thank Zhen Tao, Dr. Fabijan Pavošević, Alexander Soudackov, Benjamin Rousseau, Patrick Schneider, Dr. Saswata Roy, and Prof. John Tully for useful discussions. This work was supported by the National Science Foundation Grant No. CHE-1954348.

Supporting Information

The Supporting Information is available free of charge on the ACS Publications website: Additional computational details and tests of NEO-MSDFT approaches.

References

- 1. Cha, Y.; Murray, C. J.; Klinman, J. P. Hydrogen Tunneling in Enzyme Reactions. *Science* **1989,** *243*, 1325-1330.
- 2. Hammes-Schiffer, S. Hydrogen Tunneling and Protein Motion in Enzyme Reactions. *Acc. Chem. Res.* **2006**, *39*, 93-100.
- 3. Richardson, J. O.; Pérez, C.; Lobsiger, S.; Reid, A. A.; Temelso, B.; Shields, G. C.; Kisiel, Z.; Wales, D. J.; Pate, B. H.; Althorpe, S. C. Concerted Hydrogen-bond Breaking by Quantum Tunneling in the Water Hexamer Prism. *Science* **2016**, *351*, 1310.
- 4. Habershon, S.; Manolopoulos, D. E.; Markland, T. E.; Miller, T. F., III. Ring-polymer Molecular Dynamics: Quantum Effects in Chemical Dynamics from Classical Trajectories in An Extended Phase Space. *Annu. Rev. Phys. Chem.* **2013**, *64*, 387-413.
- 5. Litman, Y.; Richardson, J. O.; Kumagai, T.; Rossi, M. Elucidating the Nuclear Quantum Dynamics of Intramolecular Double Hydrogen Transfer in Porphycene. *J. Am. Chem. Soc.* **2019**, *141*, 2526-2534.
- 6. Vaillant, C. L.; Wales, D. J.; Althorpe, S. C. Tunneling Splittings in Water Clusters from Path Integral Molecular Dynamics. *J. Phys. Chem. Lett.* **2019**, *10*, 7300-7304.
- 7. Meyer, H. D.; Manthe, U.; Cederbaum, L. S. The Multi-configurational Time-dependent Hartree Approach. *Chem. Phys. Lett.* **1990**, *165*, 73-78.
- 8. Beck, M. H.; Jäckle, A.; Worth, G. A.; Meyer, H.-D. The Multiconfiguration Time-dependent Hartree (MCTDH) Method: A Highly Efficient Algorithm for Propagating Wavepackets. *Phys. Rep.* **2000**, *324*, 1-105.

- 9. Hammer, T.; Coutinho-Neto, M. D.; Viel, A.; Manthe, U. Multiconfigurational Time-dependent Hartree Calculations for Tunneling Splittings of Vibrational States: Theoretical Considerations and Application to Malonaldehyde. *J. Chem. Phys.* **2009**, *131*, 224109.
- 10. McCoy, A. B. Diffusion Monte Carlo Approaches for Investigating the Structure and Vibrational Spectra of Fluxional Systems. *Int. Rev. Phys. Chem.* **2006**, *25*, 77-107.
- 11. Wang, Y.; Braams, B. J.; Bowman, J. M.; Carter, S.; Tew, D. P. Full-dimensional Quantum Calculations of Ground-state Tunneling Splitting of Malonaldehyde using An Accurate Ab Initio Potential Energy Surface. *J. Chem. Phys.* **2008**, *128*, 224314.
- 12. Houston, P.; Conte, R.; Qu, C.; Bowman, J. M. Permutationally Invariant Polynomial Potential Energy Surfaces for Tropolone and H and D Atom Tunneling Dynamics. *J. Chem. Phys.* **2020**, *153*, 024107.
- 13. Webb, S. P.; Iordanov, T.; Hammes-Schiffer, S. Multiconfigurational Nuclear-electronic Orbital Approach: Incorporation of Nuclear Quantum Effects in Electronic Structure Calculations. *J. Chem. Phys.* **2002**, *117*, 4106-4118.
- 14. Pavošević, F.; Culpitt, T.; Hammes-Schiffer, S. Multicomponent Quantum Chemistry: Integrating Electronic and Nuclear Quantum Effects via the Nuclear–Electronic Orbital Method. *Chem. Rev.* **2020**, *120*, 4222-4253.
- 15. Pak, M. V.; Hammes-Schiffer, S. Electron-proton Correlation for Hydrogen Tunneling Systems. *Phys. Rev. Lett.* **2004**, *92*, 103002.
- 16. Pak, M. V.; Swalina, C.; Webb, S. P.; Hammes-Schiffer, S. Application of the Nuclear-electronic Orbital Method to Hydrogen Transfer Systems: Multiple Centers and Multiconfigurational Wavefunctions. *Chem. Phys.* **2004**, *304*, 227-236.
- 17. Skone, J. H.; Pak, M. V.; Hammes-Schiffer, S. Nuclear-electronic Orbital Nonorthogonal Configuration Interaction Approach. *J. Chem. Phys.* **2005**, *123*, 134108.
- 18. Pak, M. V.; Chakraborty, A.; Hammes-Schiffer, S. Density Functional Theory Treatment of Electron Correlation in the Nuclear–Electronic Orbital Approach. *J. Phys. Chem. A* **2007**, *111*, 4522-4526.
- 19. Brorsen, K. R.; Yang, Y.; Hammes-Schiffer, S. Multicomponent Density Functional Theory: Impact of Nuclear Quantum Effects on Proton Affinities and Geometries. *J. Phys. Chem. Lett.* **2017**, *8*, 3488-3493.
- 20. Yang, Y.; Brorsen, K. R.; Culpitt, T.; Pak, M. V.; Hammes-Schiffer, S. Development of a Practical Multicomponent Density Functional for Electron-proton Correlation to Produce Accurate Proton Densities. *J. Chem. Phys.* **2017**, *147*, 114113.
- 21. Tao, Z.; Yang, Y.; Hammes-Schiffer, S. Multicomponent Density Functional Theory: Including the Density Gradient in the Electron-proton Correlation Functional for Hydrogen and Deuterium. *J. Chem. Phys.* **2019**, *151*, 124102.
- 22. Cembran, A.; Song, L.; Mo, Y.; Gao, J. Block-localized Density Functional Theory (BLDFT), Diabatic Coupling, and Their Use in Valence Bond Theory for Representing Reactive Potential Energy Surfaces. *J. Chem. Theory Comput.* **2009**, *5*, 2702-2716.
- 23. Gao, J.; Grofe, A.; Ren, H.; Bao, P. Beyond Kohn-Sham Approximation: Hybrid Multistate Wave Function and Density Functional Theory. *J. Phys. Chem. Lett.* **2016,** *7*, 5143-5149.
- 24. Grofe, A.; Qu, Z.; Truhlar, D. G.; Li, H.; Gao, J. Diabatic-At-Construction (DAC) Method for Diabatic and Adiabatic Ground and Excited States Based on Multistate Density Functional Theory. *J. Chem. Theory Comput.* **2017**, *13*, 1176-1187.

- 25. Skone, J. H.; Soudackov, A. V.; Hammes-Schiffer, S. Calculation of Vibronic Couplings for Phenoxyl/phenol and Benzyl/toluene Self-exchange Reactions: Implications for Proton-coupled Electron Transfer Mechanisms. *J. Am. Chem. Soc.* **2006**, *128*, 16655-16663.
- 26. Sirjoosingh, A.; Hammes-Schiffer, S. Diabatization Schemes for Generating Charge-Localized Electron-Proton Vibronic States in Proton-Coupled Electron Transfer Systems. *J. Chem. Theory Comput.* **2011**, *7*, 2831-2841.
- 27. Kubas, A.; Gajdos, F.; Heck, A.; Oberhofer, H.; Elstner, M.; Blumberger, J. Electronic Couplings for Molecular Charge Transfer: Benchmarking CDFT, FODFT and FODFTB against High-level Ab Initio Calculations. II. *Phys. Chem. Chem. Phys.* **2015**, *17*, 14342-14354.
- 28. Mao, Y.; Montoya-Castillo, A.; Markland, T. E. Accurate and Efficient DFT-based Diabatization for Hole and Electron Transfer using Absolutely Localized Molecular Orbitals. *J. Chem. Phys.* **2019**, *151*, 164114.
- 29. Ghosh, S.; Verma, P.; Cramer, C. J.; Gagliardi, L.; Truhlar, D. G. Combining Wave Function Methods with Density Functional Theory for Excited States. *Chem. Rev.* **2018**, *118*, 7249-7292.
- Shao, Y.; Gan, Z.; Epifanovsky, E.; Gilbert, A. T. B.; Wormit, M.; Kussmann, J.; Lange, 30. A. W.; Behn, A.; Deng, J.; Feng, X.; Ghosh, D.; Goldey, M.; Horn, P. R.; Jacobson, L. D.; Kaliman, I.; Khaliullin, R. Z.; Kuś, T.; Landau, A.; Liu, J.; Proynov, E. I.; Rhee, Y. M.; Richard, R. M.; Rohrdanz, M. A.; Steele, R. P.; Sundstrom, E. J.; Woodcock, H. L.; Zimmerman, P. M.; Zuev, D.; Albrecht, B.; Alguire, E.; Austin, B.; Beran, G. J. O.; Bernard, Y. A.; Berquist, E.; Brandhorst, K.; Bravaya, K. B.; Brown, S. T.; Casanova, D.; Chang, C.-M.; Chen, Y.; Chien, S. H.; Closser, K. D.; Crittenden, D. L.; Diedenhofen, M.; DiStasio, R. A.; Do, H.; Dutoi, A. D.; Edgar, R. G.; Fatehi, S.; Fusti-Molnar, L.; Ghysels, A.; Golubeva-Zadorozhnaya, A.; Gomes, J.; Hanson-Heine, M. W. D.; Harbach, P. H. P.; Hauser, A. W.; Hohenstein, E. G.; Holden, Z. C.; Jagau, T.-C.; Ji, H.; Kaduk, B.; Khistyaev, K.; Kim, J.; Kim, J.; King, R. A.; Klunzinger, P.; Kosenkov, D.; Kowalczyk, T.; Krauter, C. M.; Lao, K. U.; Laurent, A. D.; Lawler, K. V.; Levchenko, S. V.; Lin, C. Y.; Liu, F.; Livshits, E.; Lochan, R. C.; Luenser, A.; Manohar, P.; Manzer, S. F.; Mao, S.-P.; Mardirossian, N.; Marenich, A. V.; Maurer, S. A.; Mayhall, N. J.; Neuscamman, E.; Oana, C. M.; Olivares-Amaya, R.; O'Neill, D. P.; Parkhill, J. A.; Perrine, T. M.; Peverati, R.; Prociuk, A.; Rehn, D. R.; Rosta, E.; Russ, N. J.; Sharada, S. M.; Sharma, S.; Small, D. W.; Sodt, A.; Stein, T.; Stück, D.; Su, Y.-C.; Thom, A. J. W.; Tsuchimochi, T.; Vanovschi, V.; Vogt, L.; Vydrov, O.; Wang, T.; Watson, M. A.; Wenzel, J.; White, A.; Williams, C. F.; Yang, J.; Yeganeh, S.; Yost, S. R.; You, Z.-Q.; Zhang, I. Y.; Zhang, X.; Zhao, Y.; Brooks, B. R.; Chan, G. K. L.; Chipman, D. M.; Cramer, C. J.; Goddard, W. A.; Gordon, M. S.; Hehre, W. J.; Klamt, A.; Schaefer, H. F.; Schmidt, M. W.; Sherrill, C. D.; Truhlar, D. G.; Warshel, A.; Xu, X.; Aspuru-Guzik, A.; Baer, R.; Bell, A. T.; Besley, N. A.; Chai, J.-D.; Dreuw, A.; Dunietz, B. D.; Furlani, T. R.; Gwaltney, S. R.; Hsu, C.-P.; Jung, Y.; Kong, J.; Lambrecht, D. S.; Liang, W.; Ochsenfeld, C.; Rassolov, V. A.; Slipchenko, L. V.; Subotnik, J. E.; Van Voorhis, T.; Herbert, J. M.; Krylov, A. I.; Gill, P. M. W.; Head-Gordon, M. Advances in Molecular Quantum Chemistry Contained in the O-Chem 4 Program Package. Mol. Phys. 2015, 113, 184-215.
- 31. Fortenberry, R. C.; Yu, Q.; Mancini, J. S.; Bowman, J. M.; Lee, T. J.; Crawford, T. D.; Klemperer, W. F.; Francisco, J. S. Communication: Spectroscopic Consequences of Proton Delocalization in OCHCO+. *J. Chem. Phys.* **2015**, *143*, 071102.
- 32. Pavošević, F.; Culpitt, T.; Hammes-Schiffer, S. Multicomponent Coupled Cluster Singles and Doubles Theory within the Nuclear-Electronic Orbital Framework. *J. Chem. Theory Comput.* **2018**, *15*, 338-347.

- 33. Webb, S. P.; Hammes-Schiffer, S. Fourier Grid Hamiltonian Multiconfigurational Self-consistent-field: A Method to Calculate Multidimensional Hydrogen Vibrational Wavefunctions. *J. Chem. Phys.* **2000**, *113*, 5214-5227.
- 34. Dunning, T. H., Jr. Gaussian Basis Sets for Use in Correlated Molecular Calculations: 1. The Atoms Boron through Neon and Hydrogen. *J. Chem. Phys.* **1989**, *90*, 1007-1023.
- 35. Yu, Q.; Pavošević, F.; Hammes-Schiffer, S. Development of Nuclear Basis Sets for Multicomponent Quantum Chemistry Methods. *J. Chem. Phys.* **2020**, *152*, 244123.
- 36. Yang, Y.; Culpitt, T.; Hammes-Schiffer, S. Multicomponent Time-dependent Density Functional Theory: Proton and Electron Excitation Energies. *J. Phys. Chem. Lett.* **2018**, *9*, 1765-1770.
- 37. Culpitt, T.; Yang, Y.; Pavošević, F.; Tao, Z.; Hammes-Schiffer, S. Enhancing the Applicability of Multicomponent Time-dependent Density Functional Theory. *J. Chem. Phys.* **2019**, *150*, 201101.
- 38. Chai, J.-D.; Head-Gordon, M. Long-range Corrected Hybrid Density Functionals with Damped Atom-atom Dispersion Corrections. *Phys. Chem. Chem. Phys.* **2008**, *10*, 6615-6620.
- 39. Käser, S.; Unke, O. T.; Meuwly, M. Reactive Dynamics and Spectroscopy of Hydrogen Transfer from Neural Network-based Reactive Potential Energy Surfaces. *New J. Phys.* **2020**, *22*, 055002.
- 40. Hazra, A.; Skone, J. H.; Hammes-Schiffer, S. Combining the Nuclear-electronic Orbital Approach with Vibronic Coupling Theory: Calculation of the Tunneling Splitting for Malonaldehyde. *J. Chem. Phys.* **2009**, *130*, 054108.